Available online at www.sciencedirect.com
SCIENCE DIRECT
Surface Science 600 (2006) 1771–1779
SURFACE SCIENCE
www.elsevier.com/locate/susc

New interpretations of XPS spectra of nickel metal and oxides

Andrew P. Grosvenor [a,1], Mark C. Biesinger [a], Roger St.C. Smart [a,b,*], N. Stewart McIntyre [a]

[a] Surface Science Western, University of Western Ontario, London, Ont., Canada N6A 5B7
[b] Applied Centre for Structural and Synchrotron Studies (ACeSSS),[2] University of South Australia, Mawson Lakes SA 5095, Australia

Received 5 May 2005; accepted for publication 27 January 2006
Available online 17 February 2006

Abstract

A current interpretation of XPS spectra of Ni metal assumes that the main 6 eV satellite is due to a two hole $c3d^9 4s^2$ (c is a core hole) final state effect. We report REELS observation in AES at low voltages of losses (plasmons and inter-band transitions) corresponding to the satellite structures in Ni metal 2p spectra. The satellite near 6 eV is attributed to a predominant surface plasmon loss. A current interpretation of Ni 2p spectra of oxides and other compounds is based on charge transfer assignments of the main peak at 854.6 eV and the broad satellite centred at around 861 eV to the cd^9L and the unscreened cd^8 final-state configurations, respectively (L is a ligand hole). Multiplet splittings have been shown to be necessary for assignment of Fe 2p and Cr 2p spectral profiles and chemical states. The assignments of Ni 2p states are re-examined with intra-atomic multiplet envelopes applied to $Ni(OH)_2$, NiOOH and NiO spectra. It is shown that the free ion multiplet envelopes for Ni^{2+} and Ni^{3+} simulate the main line and satellite structures for $Ni(OH)_2$ and NiOOH. Fitting the NiO Ni 2p spectral profile is not as straightforward as the hydroxide and oxyhydroxide. It may involve contributions from inter-atomic, non-local electronic coupling and screening effects with multiplet structures significantly different from the free ions as found for MnO. A scheme for fitting these spectra using multiplet envelopes is proposed.

Keywords: Nickel; Metals; Oxides; X-ray photoelectron spectroscopy

1. Introduction

X-ray photoelectron spectroscopy (XPS) has been extensively used in studies of the surface chemistry of metals, alloys, oxides and hydroxides with particular reference to oxidation, corrosion and chemical attack including acid dissolution (e.g. [1–3]). Nickel has assumed some increased prominence with its recent use in high temperature corrosion-resistant alloys and their reaction products (e.g. [4]). The assignment and quantitation of different surface chemical states of nickel in systems like these is potentially of considerable value in understanding and control of corrosion and dissolution. In principle, the oxidation states of nickel in the surface region can be determined from the binding energies (BE) and their chemical shifts in XPS spectra. Previous research has supported assignment of BEs of 852.6, 854.6 and 856.1 eV to Ni $2p_{3/2}$ XPS spectra for Ni^0, Ni^{2+} and Ni^{3+}, respectively in oxidized Ni, oxides, hydroxides and oxyhydroxides (e.g. [3,5,6]). This assignment can be compromised by the complex main line splitting due to multiplet contributions in oxides and by satellite structures at higher BEs particularly in the most intense Ni 2p spectra where broad maxima and extended satellite structures are often measured.

The literature on the electronic structure, theoretical models and energy loss spectroscopy (ELS) of Ni metal and NiO has recently been comprehensively reviewed by Hagelin-Weaver et al. [7,8]. They have also extensively examined alternative assignments of ELS features based

* Corresponding author. Address: Applied Centre for Structural and Synchrotron Studies (ACeSSS), University of South Australia, Mawson Lakes SA 5095, Australia. Tel.: +61 883023353; fax: +61 883023683.
E-mail address: Roger.Smart@unisa.edu.au (R.St.C. Smart).
[1] Now at: Gunning/Lemieux Chemistry Centre, University of Alberta, Edmonton, Alta., Canada T6G 2G2.
[2] Applied Centre for Structural and Synchrotron Studies, Division of Information Technology, Engineering and Environment.

0039-6028/$ - see front matter © 2006 Elsevier B.V. All rights reserved.
doi:10.1016/j.susc.2006.01.041

on both theoretical predictions and experimental behaviour. It is useful to relate this information to the core level XPS assignments of features in nickel metal and oxides.

Beginning with nickel metal ELS, they suggest that more intense features at 6.0 and 9.5 eV are due to surface and bulk plasmon losses respectively with weaker intra- and inter-band transitions at 3.7 and 7.1 eV. In XPS spectra, the well-known satellite ~6 eV above the main emission line for Ni $2p_{3/2}$ (at 852.6 eV) has previously been assigned (e.g. [9]) to a two hole $c3d^9 4s^2$ (c is a core hole) final state effect because optical and ELS experiments at that time had failed to show any structure near 6 eV and that plasmon losses could not therefore explain this satellite. We have re-examined these measurements and conclusions to relate recent ELS evidence to the interpretation of XPS core level spectra. We report that both reflection electron ELS (REELS) and Ni $2p_{3/2}$ spectra do show energy losses corresponding to surface and bulk plasmons with evidence also for weaker loss features in satellite structures of the Ni $2p_{3/2}$ spectra likely to be associated with final state effects as suggested by Hagelin-Weaver et al. [7,8].

In recent literature, the assignment of Ni $2p_{3/2}$ spectra of oxides and other compounds is based on charge transfer assignments of the main peak (at 854.6 eV in NiO) and the broad satellite (centred at ~861 eV in NiO) to the cd^9L and the unscreened cd^8 final-state configurations respectively (L is a ligand hole) (e.g. [5,9]). The same model has been previously accepted to explain main line and satellite profiles in 2p spectra of Cu and Mn oxides [9]. Quantum chemical cluster model calculations for NiO_6 [10] confirm the lowest final state with cd^9L character. A satellite arising from the overlap of the frozen ground state (with the core electron removed) and the unscreened final state of mainly cd^8 character is shifted 9.5 eV from the main peak. A second satellite with predominantly $cd^{10}L^2$ character is found shifted 6.0 eV to higher BE. This simulation produces a single peak for the main emission. Adding the six extra (frozen) NiO_6 clusters to give a Ni_7O_{36} cluster [10] now produces an additional peak on the high BE side of the main line due to a screening process by an electron that does not come from the oxygen ligands in the central NiO_6 cluster but from a neighbouring NiO_6 unit. These calculations have produced the extra peak, normally attributed to defects (e.g. Ni^{3+}), as intrinsic to the bulk NiO although the authors note that its intensity is strongly affected by defects. Extension of these simulations [11] using multiple clusters and ligand charge transfer has been shown to reproduce the complex multiplet structure in the Ni 2p spectrum. However, quantum chemical simulation [12] of 2p spectra for MnO, with complex satellite structure similar to NiO, has shown that these features can be produced without invoking charge transfer. In particular, the simulation produces a split main peak and two satellites at higher BE of similar form to the Mn 2p spectra (and to many Ni 2p spectra (e.g. [3,5])). This ab initio calculation includes relativistic electron correlation from both inter- and intra-atomic electronic interactions without any ad hoc empirical parameters. This work demonstrates that coupling of many-electron angular momenta (AM) and recoupling of high spin, open d-shell electrons, going beyond exchange coupling of open p-shell with fixed d-shell coupling, is essential for simulation of the complex Mn^{2+} 2p structure. It also shows that it is difficult to assign a single 2p BE (or chemical shift) to each ionic state of Mn or, by implication, other transition metal ion species. A multicomponent spectral envelope is necessary for each ion. Hagelin-Weaver et al. [7,8] have also examined energy losses in NiO spectra again extensively correlating assignments of ELS features based on both theoretical predictions and experimental behaviour. They conclude that there are more major losses at 4.3, 7.4 and 18.6 eV due to intra-and inter-band transitions with a bulk plasmon loss at 22.0 eV.

In practice, a simpler fit to the overall multiplet and satellite envelope for each oxidation state of nickel may be a requirement for quantitation. This view is supported by other recent research. The central importance of intra-atomic multiplet structures in fitting 2p spectra from Fe and Cr oxides has already been demonstrated [13,14]. A practical scheme for the fitting procedure has been described for each ionic state based on the Gupta and Sen (GS) calculations [15,16]. It is recognized that these multiplet components do not include inter-atomic AM coupling contributions or relativistic effects. Nevertheless, these free ion, intra-atomic multiplet calculations do include the most important intra-atomic (including spin–orbit) coupling and have successfully simulated the spectral envelopes necessary for interpretation of the Fe^{2+}, Fe^{3+} [13] and Cr^{2+}, Cr^{3+}, Cr^{5+} states [14]. They have also provided a relatively simple, practical means of resolving the different oxidation states of these metals.

In this paper, we examine the extension of these multiplet fitting envelopes to Ni 2p spectra from model compounds of both Ni^{2+}, in $Ni(OH)_2$ and NiO, and Ni^{3+} in γ-NiOOH and β-NiOOH.

2. Experimental

2.1. Materials

Nickel metal was sourced from Puratronic (Alfa Aesar, Mass, USA with 99.995% purity. It was prepared for REELS examination in the Auger microscope by first cleaning the surface using an Ar ion sputter beam and examining the surface oxide concentration, based on the O KLL signal, for extinction. At this point no remaining C could be detected on the surface.

XPS spectra from two sources of $Ni(OH)_2$ were recorded. Nickel hydroxide powder (61% Ni) was purchased from Alfa Aesar (Mass, USA). α-$Ni(OH)_2$ was supplied by Inco Limited. It was characterized by X-ray diffraction from the (003) peak areas compared with the (001) peak area of β-$Ni(OH)_2$ and found to be 92% α-phase.

γ-NiOOH, also supplied by Inco Limited, was made by oxidation of the α-$Ni(OH)_2$ It was characterized by X-ray diffraction from the (0 0 3) peak areas compared with the (0 0 1) peak area of β-NiOOH and found to be 98% γ-phase.

β-NiOOH was made by the oxidation of $Ni(NO_3)_2$ solution with bromine in aqueous KOH keeping the temperature below 20 °C in an ice bath. A black powder of mixed Ni(II)/Ni(III) was obtained. It is known that β-NiOOH readily reduces to $Ni_3O_2(OH)_4$ in ambient conditions [17]. It was characterized by FTIR as a KBr pellet giving spectra corresponding to NiOOH in the data base.

Nickel oxide powder with 99.998% purity was obtained from Puratronic (Alfa Aesar, Mass, USA).

2.2. Instrumental analysis

The nickel reflection electron energy loss spectroscopy (REELS) spectra were recorded in a PHI 660 Auger electron spectrometer. Beam energies between 200 and 3000 eV were examined.

All oxide samples were analysed in a Kratos Axis Ultra XPS. A monochromatic Al Kα X-ray source was used for all samples, along with pressures in the analysis chamber of 10^{-6}–10^{-7} Pa. The resolution function of the instrument has been found to have a width of 0.35 eV using the silver Fermi edge. To control charging of the samples, the charge neutralizer filament was used during all experiments. The Ni metal sample was sputter cleaned under vacuum (4 kV, 15 mA) to remove any oxides that had formed on the surface and then annealed at 600 °C so as to remove any point defects that may have been formed during sputtering. The Ni oxide, oxyhydroxide and hydroxide samples were all prepared and transferred into the XPS under Ar to produce pristine surfaces for analysis.

The conditions used for all of the survey scans were as follows: energy range 1100–0 eV, pass energy 160 eV, step size 0.7 eV, sweep time 180 s and X-ray spot size 700 × 400 μm. For the high-resolution spectra an energy range of 40–20 eV was used, depending on the peak being examined, with a pass energy of 10 eV and a step size of 0.05 eV.

All spectra were first analysed using the CasaXPS software [18]. Peak shifts due to any apparent charging were normalized with the C 1s peak set to 284.8 eV. After calibration, the background from each spectrum was subtracted using a Shirley-type background to remove most of the extrinsic loss structure [19]. All survey scans were analysed to determine the stoichiometry of the compound by using the appropriate sensitivity factors and to determine the amount of adventitious carbon and contaminants present.

2.3. Analysis of multiplet splitting using nickel free ion states

The Ni $2p_{3/2}$ envelope from compounds containing a high-spin Ni cation was fit using peaks corresponding to the GS multiplets and shake-up-related satellites. The GS-calculated envelopes for the Ni $2p_{3/2}$ multiplets of Ni^{2+} and Ni^{3+} are shown in Fig. 1. The calculated envelope has been fit, as in previous fits to Fe and Cr envelopes [10,11] using the minimum number of components (6) to reproduce the envelope with minimal residuals as evident in Fig. 1. Gaussian (70%)—Lorentzian (30%) profiles were used for each component. The full set of relative peak positions, FWHM and % contributions for each of Ni^{2+} and Ni^{3+} is given in Table 1. The FWHM range used (1.1–1.5 eV) was chosen based on the use of a similar range by previous authors [20,21]. As with the Fe and Cr GS multiplet fits [13,14], it is necessary to include an additional minor contribution in the region between the main line multiplets and the related satellites. From the work of Hagelin-Weaver et al. [7,8], it appears likely that this broad band may arise from the combined losses at 4.3 eV, 6.0 and 7.4 eV due to intra-and inter-band transitions allowed by breakdown of dipole selection rules in polycrystalline samples with delocalized electrons.

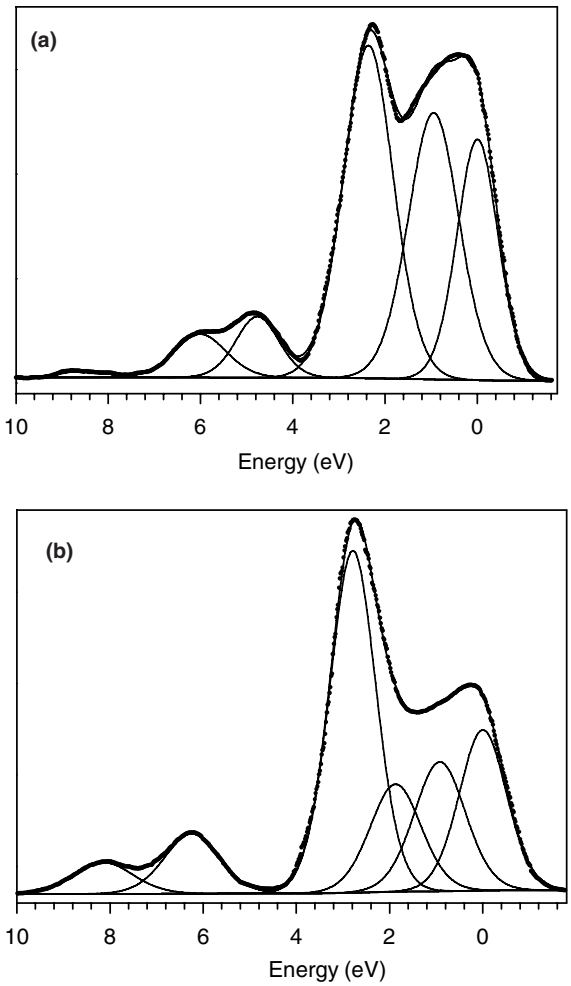

Fig. 1. Gupta and Sen multiplet envelopes (Table 1) for (a) Ni(II) and (b) Ni(III) free ions.

In both Ni^{2+} and Ni^{3+} cases, it is clear that it is difficult to assign a single BE, even as a main peak centre of gravity (CG), to these chemical states. Nevertheless, it appears that

Table 1
Relative peak positions, FWHM and % contributions for Ni^{2+} and Ni^{3+} GS envelopes

Species	Peak label	*E* (eV)	FWHM (eV)	% Contribution
Ni^{2+}	1	0.0	1.1	21.9
	2	1.0	1.3	29.9
	3	2.4	1.3	36.9
	Satellite 1	4.8	1.1	5.8
	Satellite 2	6.0	1.3	4.9
	Satellite 3	8.5	1.1	0.6
Ni^{3+}	1	0.0	1.2	18.7
	2	1.0	1.3	16.4
	3	1.9	1.3	13.6
	4	2.8	1.2	38.8
	Satellite 1	6.3	1.4	8.0
	Satellite 2	7.8	1.5	4.5

the Ni^{3+} state has a predominance of intensity at higher BE in the main line. This is consistent with the observation of Ni^{3+} growth in the K-doped oxidized Ni(1 1 0) experiments of Carley et al. [5] and the quantum calculations for defect structures [10] where intensity increases in a multi-peak envelope near 856.1 eV.

The experimental spectra were fit using components and intensities (peak areas) similar to those in Fig. 1 and Table 1 except that the FWHM of the main peaks were allowed to vary (up to 1.5 eV) to optimize the fit. A single broad, weak peak (FWHM 3.2–3.4 eV) was also added at higher BE (shifted ~12 eV) to complete the fits. This may be due to truncation error in background subtraction or to other extended losses beyond 8.5 eV [7,8]. The fits were adequate for $Ni(OH)_2$ and NiOOH compounds. After the $2p_{3/2}$ envelope was fitted using the above method, the main peak CG was determined using the GS multiplets only.

3. Results

3.1. Nickel metal spectra

Fig. 2 shows the Ni $2p_{3/2}$ XPS spectrum from clean nickel metal with the two obvious satellite intensities fit by broad peaks (FWHM 2.5 eV) with BE near 3.7 eV (minor) and 6.0 eV (major) above the main line at 852.6 eV.

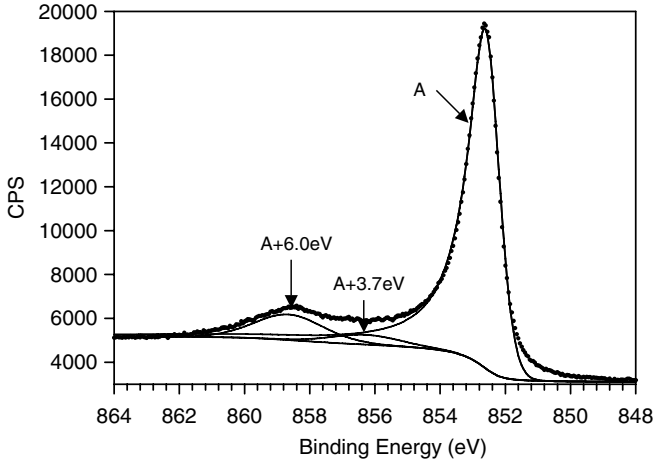

Fig. 2. Ni $2p_{3/2}$ spectrum from clean nickel metal.

Fig. 3 gives the REELS spectra recorded at 0.2 keV beam voltage for clean nickel. This voltage is represented because it gave the best resolution of loss features for surface sensitivity on the PHI 660 instrument. At higher energies, the elastic peak overlapped the lower energy loss peaks. The 5.5 and 7.0 eV loss peaks increased in intensity

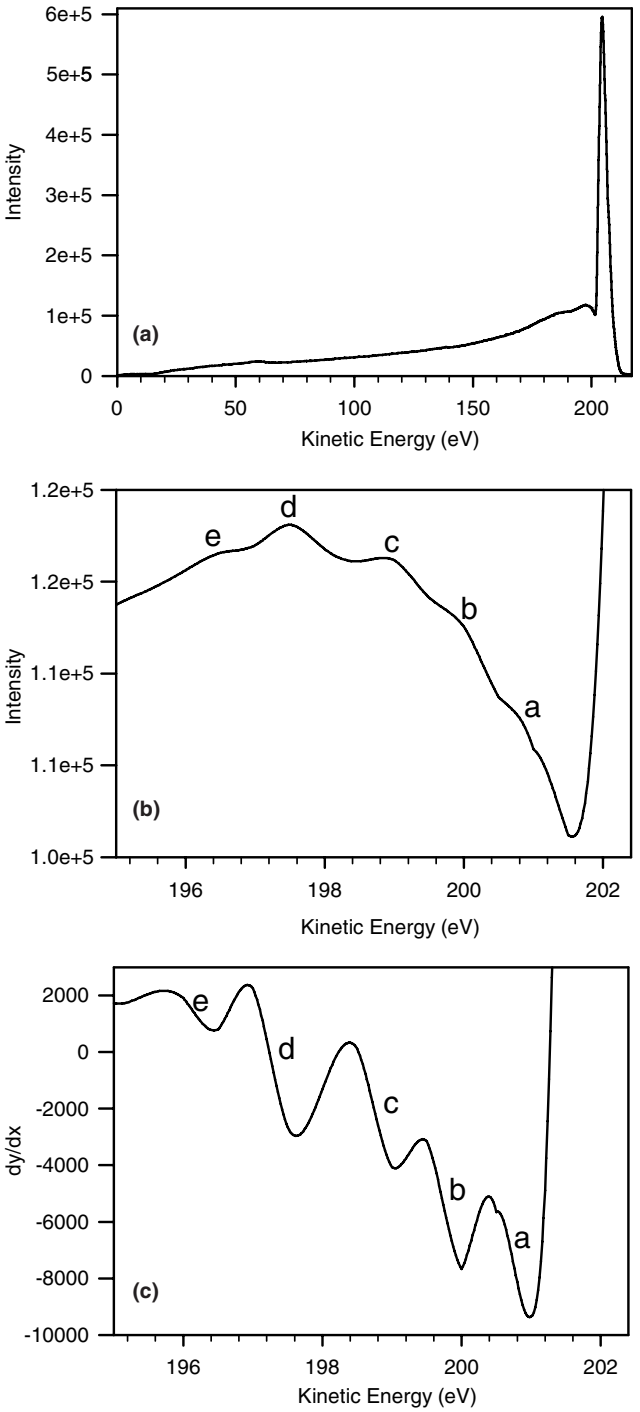

Fig. 3. REELS Ni metal spectra at 0.2 kV beam voltage. (a) Elastic peak with loss structure, (b) expanded region of loss structure below elastic peak, (c) first derivative spectrum of loss structure.

and sharpness at lower voltages (100–200 eV), an observation also made in the ELS work of Hagelin-Weaver et al. [7,8] for their 6 eV peak, suggesting a surface rather than bulk process. Fig. 3a shows the main elastic peak at 204.5 eV with obvious loss structure at lower kinetic energies. Fig. 3b is the region close to the main peak. Analysis of the extrinsic losses at 200 eV using the Tougaard QUASES-XS-REELS program 2.1 [22] produces a very broad, continuous envelope across 200–190 eV. The modeling of the extrinsic losses does not seem to have been done in previous REELS interpretation making identification of the positions of loss maxima less certain. Even with this correction, the attributions of specific loss peak energies in this and other work (see Table 1 in Ref. [7]) are difficult to deconvolute. Broader peaks may contain more than one origin. Recognising this limitation, superimposed on this broad extrinsic loss peak we appear to distinguish loss peaks near 3.5 eV (a), 4.5 eV (b), 5.5 eV (c), 7.0 eV (d) and 8.5 eV (e). The first derivative spectrum in Fig. 3c shows the positions of these peaks more clearly. Peaks (c) and (d) are the most prominent corresponding to losses across the 6 eV satellite in the Ni $2p_{3/2}$ spectrum from clean nickel metal. Similar REELS loss structures are observed for nickel metal, with decreasing intensity relative to the main reflection, up to 1000 eV beam energies. It is noted that no loss peaks were observed for a NiO(1 0 0) single crystal face at 500 eV beam energy.

3.2. Nickel hydroxide and oxyhydroxide spectra

The XPS spectra from the two nickel hydroxide sources gave identical multiplet fits without changing any of the parameters in Table 1. Fig. 4 shows the Ni $2p_{3/2}$ spectrum from $Ni(OH)_2$ which is well fit with the GS Ni^{2+} multiplet set with the additional broad loss peak at 857.9 eV. This fit does not require any contributions from any other Ni states (see below). The FWHM of the main line contributions are 1.2, 1.4 and 1.5 eV, respectively with increasing BE.

Fig. 5 shows the Ni $2p_{3/2}$ spectrum from γ-NiOOH which is well fitted with the GS Ni^{3+} multiplet set with the additional broad surface peak at 858.1 eV. This fit does not require any contributions from any other Ni states including Ni^{2+}. The FWHM of the four main line contributions are 1.4, 1.5, 1.4 and 1.4 eV, respectively with increasing BE.

Fig. 6 shows the Ni $2p_{3/2}$ spectrum from β-NiOOH This spectrum is closely similar to that reported previously by Moroney et al. [6] for β-NiOOH after some dehydration at 200 °C This oxyhydroxide is a mixed Ni^{2+}/Ni^{3+} phase as noted above. The $OH^-:O^{2-}$ ratio from O 1s spectra was 2:1 confirming the decomposition to $Ni_3(OH)_4O_2$. It is well fit with the combination of GS Ni^{2+} and Ni^{3+} multiplet sets in 1:2 ratio again with the additional broad loss peak at 858.1 eV. It is important to emphasise here that we are not using 12 independent components in this fit but two sets of 6 components in which only the *relative* proportion

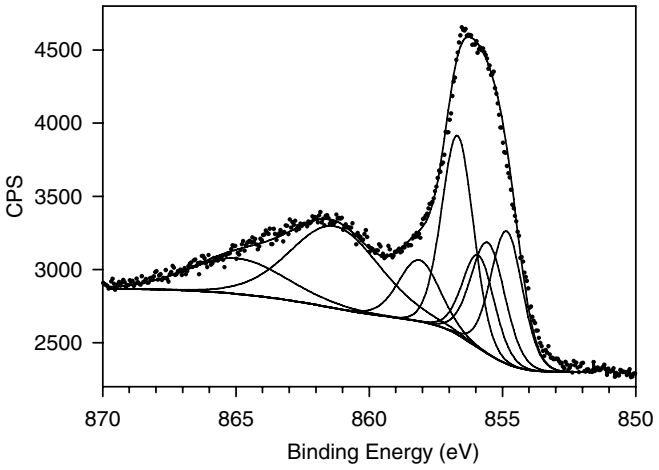

Fig. 5. Ni $2p_{3/2}$ spectrum of γ-NiOOH fitted with Ni(III) multiplet envelope.

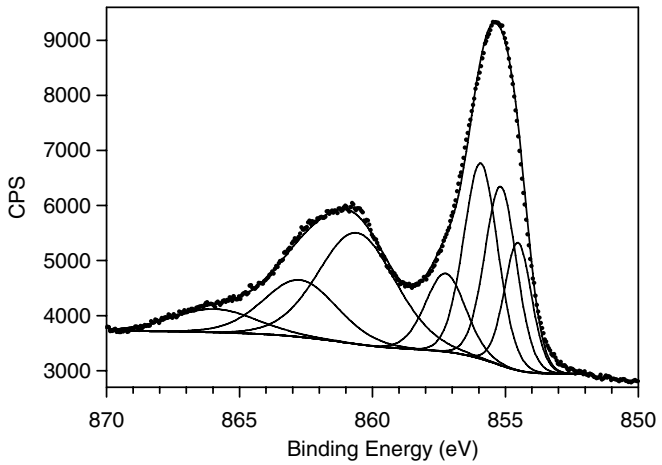

Fig. 4. Ni $2p_{3/2}$ spectrum from $Ni(OH)_2$ fitted with Ni(II) multiplet envelope.

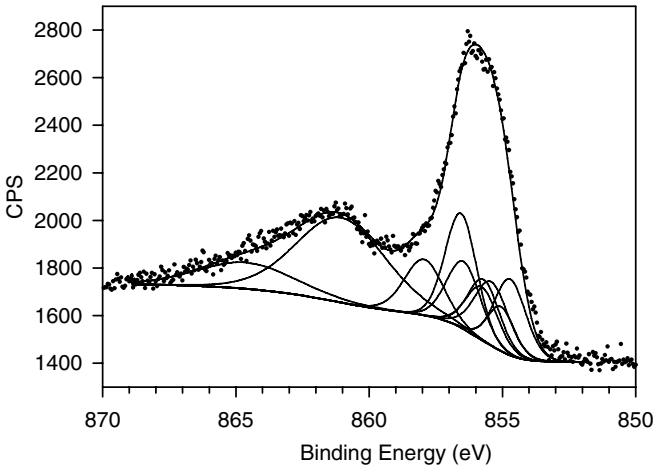

Fig. 6. Ni $2p_{3/2}$ spectrum of β-NiOOH fitted with Ni(II) and Ni(III) multiplet envelopes.

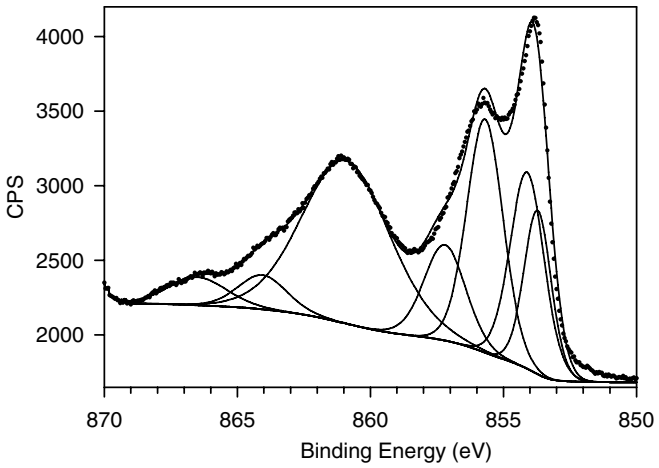

Fig. 7. NiO fitted with Ni(II) multiplet structure allowing variation of the multiplet spacings.

of the two sets is allowed to vary giving the Ni^{2+}/Ni^{3+} ratio.

3.3. NiO spectra

The Ni $2p_{3/2}$ spectra from polycrystalline NiO are closely similar to those reported previously for NiO powders prepared by sintering above 1000 °C [3]. This spectrum cannot be satisfactorily fit with the unaltered Ni^{2+} multiplets in Fig. 1a or with FWHM variation alone. A satisfactory fit can only be achieved by allowing variation in the BE positions of the multiplet contributions to the main peak. An illustration of one such fit is given in Fig. 7. Here, the spacings of the three peaks making up the main peak are altered from 0.95 and 1.4 eV to 0.5 and 1.6 eV, respectively. As with Fe and Cr 2p spectra, there is also a broad peak associated with other intrinsic losses at a higher binding energy than the main peak multiplets. In all of these cases, this contribution is necessary to model the valley between the main peak and the satellite structures and is consistent with the inter-band losses attributed by Hagelin-Weaver et al. [7,8].

4. Discussion

4.1. Nickel metal spectra

The REELS results in Fig. 3 show that a variety of loss processes can be measured in the clean nickel metal surface. Comparing our loss energies with the careful analysis of alternative assignments by Hagelin-Weaver et al. [7,8], the first loss near 3.5 eV is likely to be associated with the Ni 3d (high spin) to Ni 4s (low spin) transition in surface atoms. ELS peaks in the 4.2–4.8 eV range have been attributed to either inter-band transitions (e.g. [23]) or surface plasmons [24] and there is convincing evidence for surface loss processes at 4.0–4.5 eV in optical and dielectric function data (summarized in Table 2, Ref. [7]). The larger loss peak near 5.5 eV may be the surface plasmon assigned by Hagelin-Weaver et al. [7,8] at 6.0 eV in their work. They assign a peak near 7.0 eV to a Ni 3d (low spin) to Ni 4p (low spin) transition in surface atoms. The weaker 8.5 eV peak may be due to a multiple or combination of these loss peaks or to a bulk plasmon assigned by Hagelin-Weaver et al. [7] at 9.0 eV.

In the comprehensive summary and interpretation of ELS and optical (with dielectric function) data on Ni metal by Hagelin-Weaver et al. [7], convincing evidence for a surface plasmon loss near 6 eV is presented although, as they note, the reported peak position varies up to 8.3 eV in more than 10 reports. At lower primary beam energies (<200 eV), the peak centre shifts towards lower energy loss values closer to 6 eV while at higher beam energies, the intensity of a higher energy loss peak increases and shifts towards values above 9 eV. These observations are consistent with our REELS measurements. Other papers have described trends in measurements of EELS for different transition metals consistent with surface plasmon losses. The early paper by Robins and Swan [25] suggested that the peaks at loss energies less than 10 eV may be due to plasmons but their beam excitation energy was high and the peaks very broad. Ingram et al. [26] extended this work confirming the assignment to a surface plasmon near 6.0 eV. Kemeny and Shevchik [27] examined the XP spectra of Ni in a Ni90Zn10 alloy and suggested that, if the Ni satellite is from plasmon loss, it should also be found in the Zn $2p_{3/2}$ spectrum. They conclude that it is not but do not discuss a small broad satellite above 6 eV separation energy. A satellite peak is present in Zn metal with similar loss energy to that found in the Ni90Zn10 alloy albeit with lower intensity than satellites in Ni or Co. It is also noted that a two-hole final state effect should result in an asymmetric satellite profile due to Doniach-Sunjic processes [28]. The profile in Fig. 2 is, in our view, extended but not asymmetric.

It remains possible that the 3.5 eV peak is also a surface plasmon rather than a shake-up peak. This interpretation has been followed by Grosvenor et al. [29] in their paper on XP spectra of Co metal and phosphides. They also measured REELS peaks at 3.0 and 5.0 eV from Co metal. Their evidence suggests that both are surface plasmons differing only in the depth at which the plasmon oscillation is occurring, i.e. the higher energy loss is from deeper layers but not true bulk.

Overall, the combination of these losses in Ni 2p XPS spectra gives rise to the broad peaks fit well with the 3.7 and 6.0 eV components of Fig. 2. These components are not taken to represent specific processes but are likely, on the basis of the REELS evidence, to represent both plasmon and some shake-up losses from the primary Ni 2p emission. In fact, it will be clear that it is possible to fit this extended profile with the set of 5 bands, corresponding to the 3.5, 4.5, 5.5, 7.0 and 8.0 eV loss peaks in Fig. 3. We have not done this here because it is inherently simpler and more practical to use the two peak fit shown in Fig. 2.

This suggests that the current explanation of satellite structure in Ni XP spectra should be re-examined. This theory compares initial and final states attributing the main line to $c3d^{10}4s$ and the satellite to $c3d^{9}4s^{2}$ after photoionization. The argument (and BE estimates), summarized in Hüfner [9], is that the additional Coulomb attraction due to the core hole can pull the conduction band below the Fermi level so that an additional charge is put into the 3d orbitals, i.e. $3d^{10}$ for the ground state (main line). The higher BE state is said to arise from the 3d band not being completely filled and screening is produced instead within the wide 4s band. This posits a two-hole state, core hole and 3d hole, in an excited state 6 eV above the ground state. If this is the origin of the satellite, these peaks should not be found in REELS data since no photoionization has occurred. The observation of the REELS loss peaks makes it more likely that this is the true origin of the Ni metal satellite structures. This was acknowledged by Hüfner [9] to be the most obvious explanation but it was accepted that no loss functions had previously been observed for nickel metal at that time.

4.2. Nickel hydroxide and oxyhydroxides

The fitting of these Ni 2p spectra from $Ni(OH)_2$, γ-NiOOH and β-NiOOH with relatively simple multiplet envelopes for Ni^{2+}, Ni^{3+} and their combination (respectively) suggests that inter-atomic AM interactions are not dominant in these structures. The intra-atomic GS multiplet interactions are sufficient to adequately model the complex envelopes of the Ni 2p spectra in these cases without invoking charge transfer or other final state effects.

4.3. Nickel oxide

Modelling this oxide with GS multiplet states is obviously more complex than the hydroxide and oxyhydroxide compounds. The summary in the Introduction of some relevant literature [7–12] on alternative explanations of the origin of the complex main line and satellite structures illustrates the continuing discussion on whether these features can be explained by extended multiplet interactions or require ligand charge transfer to simulate the overall emission envelope. The necessity to vary the positions of the GS AM multiplet contributions can potentially be explained in two ways.

In the quantum chemical simulation of Ni 2p XPS line shapes for NiO by van Veenendaal and Sawatsky [10], interactions of the central Ni atom (core hole c) with either neighbouring NiO_6 octahedra or with oxygen-deficient defects broadened the main line and the satellite. In these multiple cluster calculations, the lowest final state still has predominant $cd^{9}L$ character with charge transfer from the adjacent oxygen atoms. Additions to the satellite structure arise from intersite charge transfer screening and increased width of the $cd^{10}L^{2}$ states due to oxygen banding effects. The strong influence of the non-local screening effects, with contributions from $d^{n+1}d^{n-1}$ charge transfer states and associated multiplet structure, on the energies and line shapes of core-level photoemissions has been demonstrated in the calculations of Atanasov and Reinen [11]. Hence, the multiplet and satellite envelopes in Ni 2p spectra from NiO are unlikely to be fit with the free ion GS components.

Bagus et al. [12] have also shown convincingly for MnO that a complete fit to the 2p spectra can be obtained using all inter-atomic wave function mixing and coupling/recoupling AM contributions. These contributions are not included in the free ion GS intra-atomic calculations. When this is done, the complex spectra can be interpreted without explicit ligand charge transfer as in the current interpretation of the main line as the $cd^{9}L$ screened emission. In this theory, however, it is noted that the O 2p band is overlapped with the Ni 3d band in NiO UV photoemission. This suggests that inter-atomic wave function mixing is favoured in the structure contributing to the

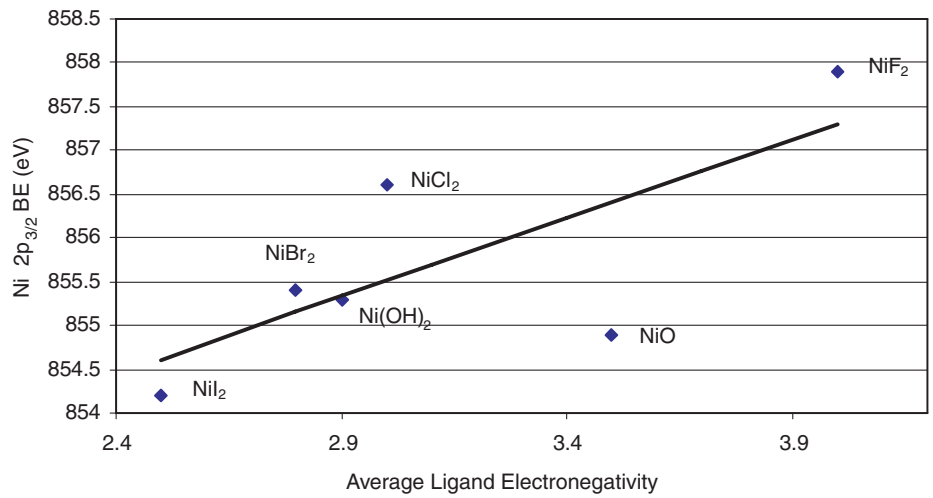

Fig. 8. Change of core Ni $2p_{3/2}$ BE (CG values) with electronegativity of the ligand.

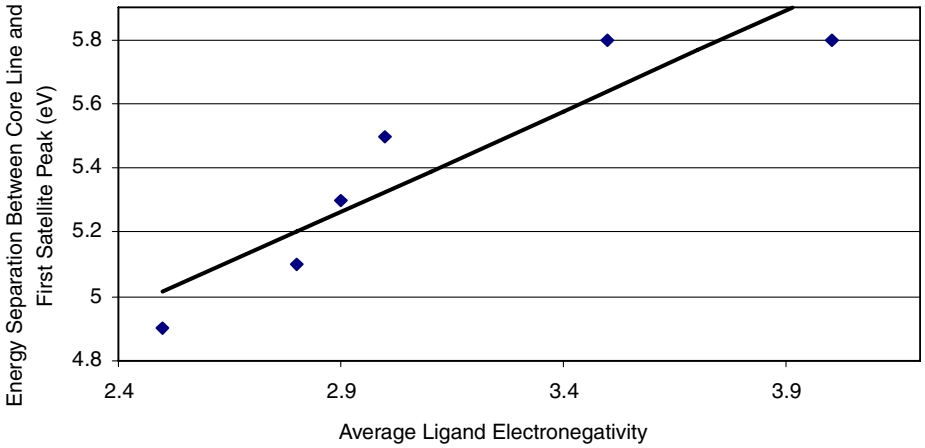

Fig. 9. BE separation between Ni $2p_{3/2}$ core line and first satellite peak with electronegativity of the ligand.

AM contributions in the Bagus et al. treatment. The origin of the emissions from the main line and satellites may only be resolved by further theoretical modelling of the NiO structure using all inter-atomic wave function mixing and coupling/re-coupling AM contributions.

Consideration of the position of the BEs resulting from the electronegativity effects of neighbouring ligands is also informative. The CG values calculated from the curve fits for $Ni(OH)_2$, NiOOH and NiO spectra are 855.3, 855.8 and 854.7 eV, respectively. An examination of the BE shifts (taken from the CGs) and main line/satellite separation with ligand electronegativity [30] is instructive (Figs. 8 and 9). These figures contain data from the samples measured here and the nickel halides (fluoride, chloride, bromide and iodide to be discussed in a subsequent paper). Fig. 9 shows a reasonable progression of satellite displacement with increasing ligand electronegativity from NiI_2 (2.5) through NiO (3.5) to NiF_2 (4.0). Conversely, the value for the NiO BE is aberrant in Fig. 8 compared with the other compounds. A possible reason for this might be that the BE of the Ni $2p_{3/2}$ peak does not represent the Madelung effect of the electronegativity of the ligands alone. The effect of electronegativity alone should produce a BE near 856 eV. In fact, the NiO result appears to represent the strong effect of the oxide ligands on both BE and multiplet splitting. It is likely therefore that inter-atomic wave function mixing, as proposed by Atanasov and Reinen [11] and Bagus et al. [12], shifts the true BE of the Ni 2p spectra in NiO.

5. Conclusions

REELS results at low beam energies have shown that surface plasmons and inter-band transitions can be measured in the clean nickel metal surface. The larger loss peaks near 5.5 and 7.0 eV can be attributed to plasmon losses with corresponding less-intense losses near 3.5 and 4.5 eV, respectively. The observation of the REELS loss peaks makes it likely that this is the true origin of the Ni metal satellite structures rather than the two-hole final state theory. This final state effect would not be observed in REELS spectra without photoemission.

Ni 2p spectra from $Ni(OH)_2$, γ-NiOOH and β-NiOOH are adequately fitted with relatively simple Gupta and Sen intra-atomic free ion multiplet envelopes for Ni^{2+}, Ni^{3+} and their combination respectively implying limited inter-atomic angular momenta electronic interactions. Modelling NiO with GS multiplet states is more complex than the hydroxide and oxyhydroxide compounds necessitating multiplet contributions different from the free ion GS Ni^{2+} envelope for adequate fitting. A more complete analysis may require all inter-atomic wave function mixing and coupling/re-coupling AM contributions not included in the free ion GS intra-atomic calculations. The evidence suggests that assigning nickel states from single BE values of Ni $2p_{3/2}$ spectra alone may carry significant uncertainty and may require fitting with more complete multiplet envelopes before quantitative analysis.

Acknowledgements

We thank Dr. Sridath Ramamurthy for his expert assistance with the Auger REELS measurements and Brad Kobe (Surface Science Western) for continuing discussions on nickel XPS spectra. The α-$Ni(OH)_2$ and γ-NiOOH were kindly supplied by Inco Limited, Mississauga, Ontario, Canada with thanks to Dr. Feng Zou. The considerable assistance of the reviewers with additional literature has improved the paper.

References

[1] M.W. Roberts, Adv. Catal. 29 (1980) 55.
[2] N.S. McIntyre, Corrosion and surface analysis, in: J.C. Riviere, S. Myhra (Eds.), Handbook of Surface and Interface Analysis, vol. 643, Marcel Dekker, New York, 1998.
[3] M.W. Roberts, R.St.C. Smart, J. Chem. Soc. Faraday I 80 (1984) 2957.

[4] N.S. McIntyre, R.D. Davidson, T.L. Walzak, A.M. Brennenstuhl, F. Gonzalez, S. Corrazza, Corros. Sci. 37 (1995) 1059.
[5] A.F. Carley, S.D. Jackson, J.N. O'Shea, M.W. Roberts, Surf. Sci. 440 (1999) L868–L874.
[6] L.M. Moroney, R.St.C. Smart, M.W. Roberts, J. Chem. Soc. Faraday Trans. I 79 (1983) 1769–1778.
[7] H.A.E. Hagelin-Weaver, J.F. Weaver, G.B. Hoflund, G.N. Salaita, J. Electron, Spec. Rel. Phenom. 134 (2004) 139–171.
[8] H.A.E. Hagelin-Weaver, J.F. Weaver, G.B. Hoflund, G.N. Salaita, J. Alloys, Compounds 389 (2005) 34–41.
[9] S. Hufner, Photoelectron spectroscopy, Solid State Science Series, vol. 82, Springer-Verlag, 1995 (Chapter 3 and references therein).
[10] M.A. van Veenendaal, G.A. Sawatsky, Phys. Rev. Lett. 70 (1993) 2459.
[11] M. Atanasov, D. Reinen, J. Electron, Spectrosc. Relat. Phenom. 86 (1997) 185.
[12] P.S. Bagus, R. Broer, W.A. de Jong, W.C. Nieuwpoort, F. Parmiginai, L. Sangaletti, Phys. Rev. Lett. 84 (2000) 2259.
[13] A.P. Grosvenor, B.A. Kobe, M.C. Biesinger, N.S. McIntyre, Surf. Interface Anal. 36 (2004) 1564.
[14] M.C. Biesinger, C. Brown, J.R. Mycroft, R.D. Davidson, N.S. McIntyre, Surf. Interface Anal. 36 (2004) 1550.
[15] R.P. Gupta, S.K. Sen, Phys. Rev. B 10 (1974) 71.
[16] R.P. Gupta, S.K. Sen, Phys. Rev. B 12 (1975) 15, GS II.
[17] A.F. Cotton, G. Wilkinson, Advanced Inorganic Chemistry, second ed., Interscience Wiley, New York, London, Sydney, 1966, Section 29-G-5.
[18] http://www.casaxps.com.
[19] B.S. Norgren, M.A.J. Somers, J.H.W. de Wit, Surf. Interface Anal. 21 (1994) 378.
[20] N.S. McIntyre, D.G. Zetaruk, Anal. Chem. 49 (1977) 1521.
[21] J.R. Mycroft, H.W. Nesbitt, A.R. Pratt, Geochim. Cosmochim. Acta 59 (1995) 721.
[22] QUASES-XS-REELS Version 2.1, QUASES Tougaard Inc. (Odense, Denmark). Available from: <www.quases.com>.
[23] E. Sickafus, F. Steinrisser, Phys. Rev. B 6 (1972) 3714.
[24] H.B. Koldoziej, B. Rozenfeld, Acta Phys. Pol. A 48 (1975) 765.
[25] J.L. Robins, J.B. Swan, Proc. Phys. Soc. 76 (1960) 857.
[26] J.C. Ingram, K.W. Nebesny, J.E. Pemberton, Appl. Surf. Sci. 45 (1990) 247.
[27] P.C. Kemeny, N.J. Shevchik, Solid State Comm. 17 (1975) 255.
[28] S. Doniach, M. Sunjic, J. Phys. C 3 (1970) 285.
[29] A.P. Grosvenor, S.D. Wik, R.G. Cavell, A. Mar, Inorg. Chem. 44 (2005) 8988–8998.
[30] L. Pauling, The Nature of the Chemical Bond, third ed., Cornell University Press, 1960, p. 93.